Soft Matter

ARTICLE

Supplementary Information for "Design rules for glass formation from model molecules designed by a neural-network-biased genetic algorithm"

Received 00th January 20xx,
Accepted 00th January 20xx

DOI: 10.1039/x0xx00000x

www.rsc.org/

Venkatesh Meenakshisundaram,[a] Jui-Hsiang Hung[a] and David S. Simmons[a,*]

Structural information for extremal fragility molecules

Here we provide, in Supplementary Table 1 and Supplementary Table 2, angular data required to construct rigid molecules identified to have maximal and minimal fragilities, respectively, for each n. Angles are employed in the algorithm for rigid body generation section described in the main text.

Supplementary Table 1. Azimuthal and polar angles for construction of 3-bead, 4-bead, and 6-bead rigid molecules identified to have maximal fragility.

	3rd bead		4th bead		5th bead		6th bead	
	θ	ϕ	θ	ϕ	θ	ϕ	θ	ϕ
3-bead	67.5	-	-	-	-	-	-	-
4-bead	281.25	-	326.25	0.0	-	-	-	-
6-bead	270.0	-	253.13	129.38	196.86	343.13	101.25	67.5

Supplementary Table 2. Azimuthal and polar angles for construction of 3-bead, 4-bead, and 6-bead rigid molecules identified to have minimal fragility.

	3rd bead		**4th bead**		**5th bead**		**6th bead**	
	θ	ϕ	θ	ϕ	θ	ϕ	θ	ϕ
3-bead	157.5	-	-	-	-	-	-	-
4-bead	354.38	-	185.63	331.88	-	-	-	-
6-bead	163.13	-	11.25	213.75	174.36	123.75	0.0	0.0

Results for dynamical quantities at computational timescales

In the main text we report on a number of correlations between T_g and fragility, as defined based on an extrapolation to an experimental timescale, and other dynamic and thermodynamic quantities. Supplementary Figure 1 below replicates many of the correlation figures in the main text, but employing computational timescale values of T_g and m, illustrating that the trends reported on in the main manuscript are qualitatively insensitive to this choice.

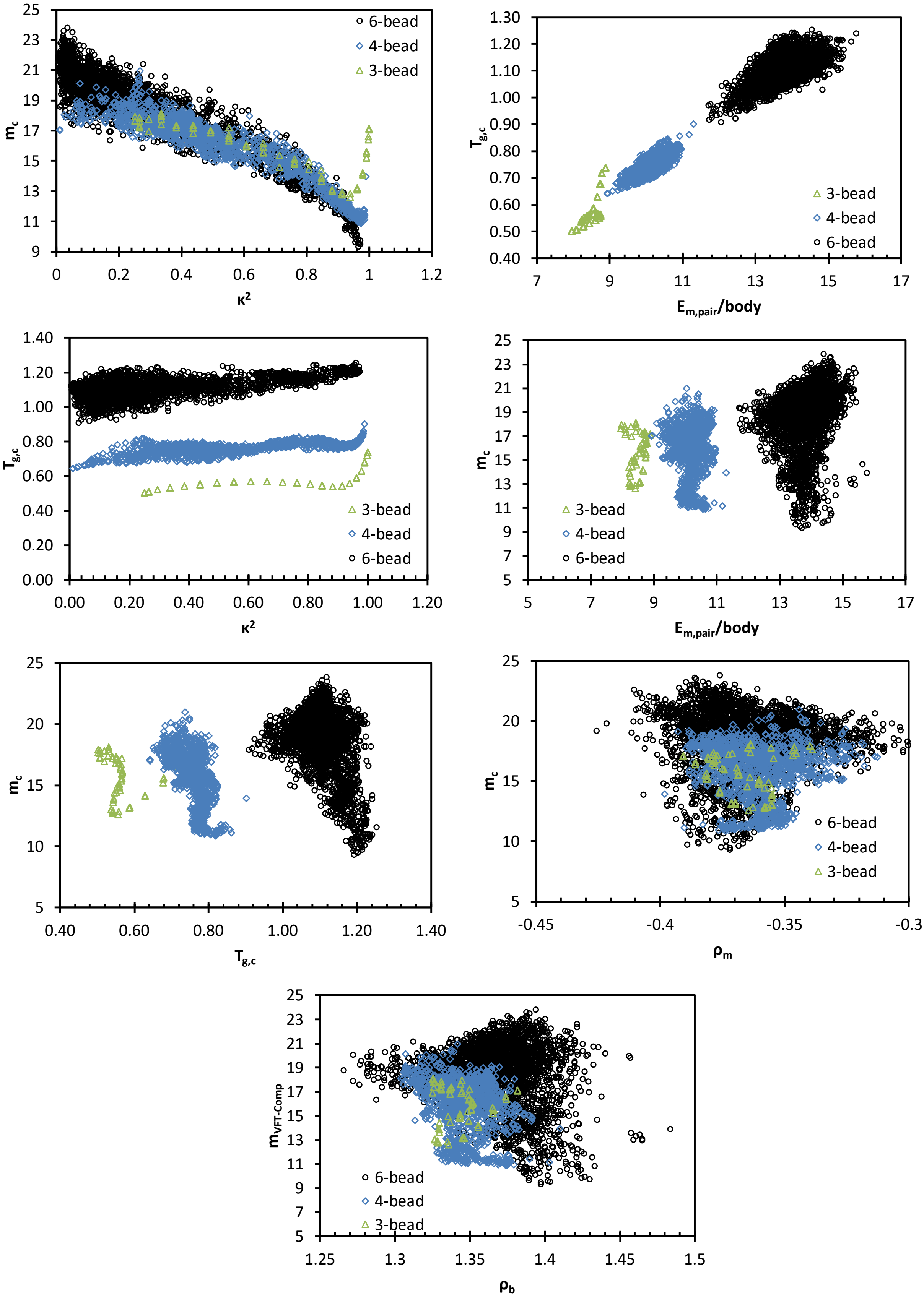

Supplementary Figure 1. Correlation diagrams shown in the main text, but for fragilities and glass transition temperatures computed at a computational timescale of 10^4 LJ time units.

Additional Supplementary Data

Below we provide data on correlations between a large range of dynamic and thermodynamic properties quantified for the systems simulated in this study. Supplementary Table 3 provides values of R^2 for second order polynomial fits between pairs of properties studied. These correlations are assessed at the level of all data involved in the study, and separately for each molecular size. We have additionally tested linear and higher order polynomial correlations for many of these pairs of quantities; due to the large volume of data, generally these modest changes in fit order do not have a large effect on the resulting value of R^2. Supplementary figures graphically depict the relationships between these quantities.

Supplementary Table 3 Correlation between various descriptors associated with glass formation behavior represented by a second order polynomial fit

Property 1	Property 2	Overall R^2	3-bead R^2	4-bead R^2	6-bead R^2
T_g, glass transition temp.	m, Kinetic fragilty	0.265	0.075	0.113	0.109
T_g	κ^2, Relative shape anisotropy	0.162	0.241	0.047	0.020
T_g	$E_{m,pair}$, slope of pair energy vs. temp	0.966	0.767	0.662	0.582
T_g	$E_{b,pair}$, intercept of pair energy vs. temp	0.972	0.705	0.526	0.499
T_g	ρ_m, slope of density vs. temp	0.168	0.769	0.656	0.497
T_g	ρ_b, intercept of density vs. temp	0.409	0.837	0.447	0.566
T_g	$E_{pair,Tg}$, extrp. pair energy at T_g	0.901	0.241	0.126	0.073
T_g	ρ_{Tg}, extrp. density at T_g	0.899	0.669	0.177	0.182
T_g	E_a, High-temp activation energy	0.914	0.900	0.240	0.513
T_g	$-\log(\tau_0)$, high-temp relaxation time	0.897	0.734	0.191	0.599
m	κ^2	0.772	0.444	0.748	0.736
m	$E_{m,pair}$	0.335	0.078	0.062	0.132
m	$E_{b,pair}$	0.325	0.091	0.050	0.252
m	ρ_m	0.055	0.058	0.049	0.069
m	ρ_b	0.115	0.084	0.050	0.135
m	$E_{pair,Tg}$	0.284	0.629	0.315	0.093
m	$\rho_{pair,Tg}$	0.393	0.111	0.268	0.346
m	E_a	0.201	0.000	0.429	0.183
m	$-\log(\tau_0)$	0.413	0.330	0.441	0.187
κ^2	$E_{m,pair}$	0.205	0.124	0.033	0.022
κ^2	$E_{b,pair}$	0.218	0.650	0.170	0.079
κ^2	ρ_m	0.011	0.152	0.022	0.030
κ^2	ρ_b	0.033	0.235	0.187	0.149
κ^2	$E_{pair,Tg}$	0.227	0.521	0.218	0.152
κ^2	$\rho_{pair,Tg}$	0.286	0.167	0.140	0.254
κ^2	E_a	0.074	0.594	0.569	0.249
κ^2	$-\log(\tau_0)$	0.292	0.275	0.435	0.093

Descriptor 1	Descriptor 2	Overall R^2	3-bead R^2	4-bead R^2	6-bead R^2
$E_{m,pair}$	$E_{b,pair}$	0.964	0.483	0.525	0.471
$E_{m,pair}$	ρ_m	0.326	0.987	0.970	0.884
$E_{m,pair}$	ρ_b	0.403	0.638	0.399	0.469
$E_{m,pair}$	$E_{pair,Tg}$	0.891	0.316	0.126	0.104
$E_{m,pair}$	$\rho_{pair,Tg}$	0.912	0.580	0.274	0.303
$E_{m,pair}$	E_a	0.896	0.476	0.352	0.414
$E_{m,pair}$	$-\log(\tau_0)$	0.899	0.664	0.168	0.598
$E_{b,pair}$	ρ_m	0.093	0.532	0.408	0.266
$E_{b,pair}$	ρ_b	0.298	0.900	0.820	0.411
$E_{b,pair}$	$E_{pair,Tg}$	0.964	0.614	0.130	0.241
$E_{b,pair}$	$\rho_{pair,Tg}$	0.879	0.423	0.037	0.037
$E_{b,pair}$	E_a	0.880	0.892	0.466	0.317
$E_{b,pair}$	$-\log(\tau_0)$	0.856	0.805	0.021	0.472
ρ_m	ρ_b	0.497	0.691	0.327	0.569
ρ_m	$E_{pair,Tg}$	0.053	0.355	0.173	0.218
ρ_m	$\rho_{pair,Tg}$	0.096	0.657	0.309	0.207
ρ_m	E_a	0.166	0.596	0.345	0.487
ρ_m	$-\log(\tau_0)$	0.206	0.761	0.217	0.461
ρ_b	$E_{pair,Tg}$	0.160	0.348	0.127	0.042
ρ_b	$\rho_{pair,Tg}$	0.119	0.574	0.152	0.028
ρ_b	E_a	0.456	0.861	0.419	0.656
ρ_b	$-\log(\tau_0)$	0.333	0.715	0.034	0.296
$E_{pair,Tg}$	$\rho_{pair,Tg}$	0.803	0.415	0.760	0.416
$E_{pair,Tg}$	E_a	0.777	0.107	0.043	0.057
$E_{pair,Tg}$	$-\log(\tau_0)$	0.705	0.569	0.214	0.096
$\rho_{pair,Tg}$	E_a	0.752	0.691	0.130	0.021
$\rho_{pair,Tg}$	$-\log(\tau_0)$	0.824	0.783	0.252	0.280
E_a	$-\log(\tau_0)$	0.846	0.752	0.004	0.447

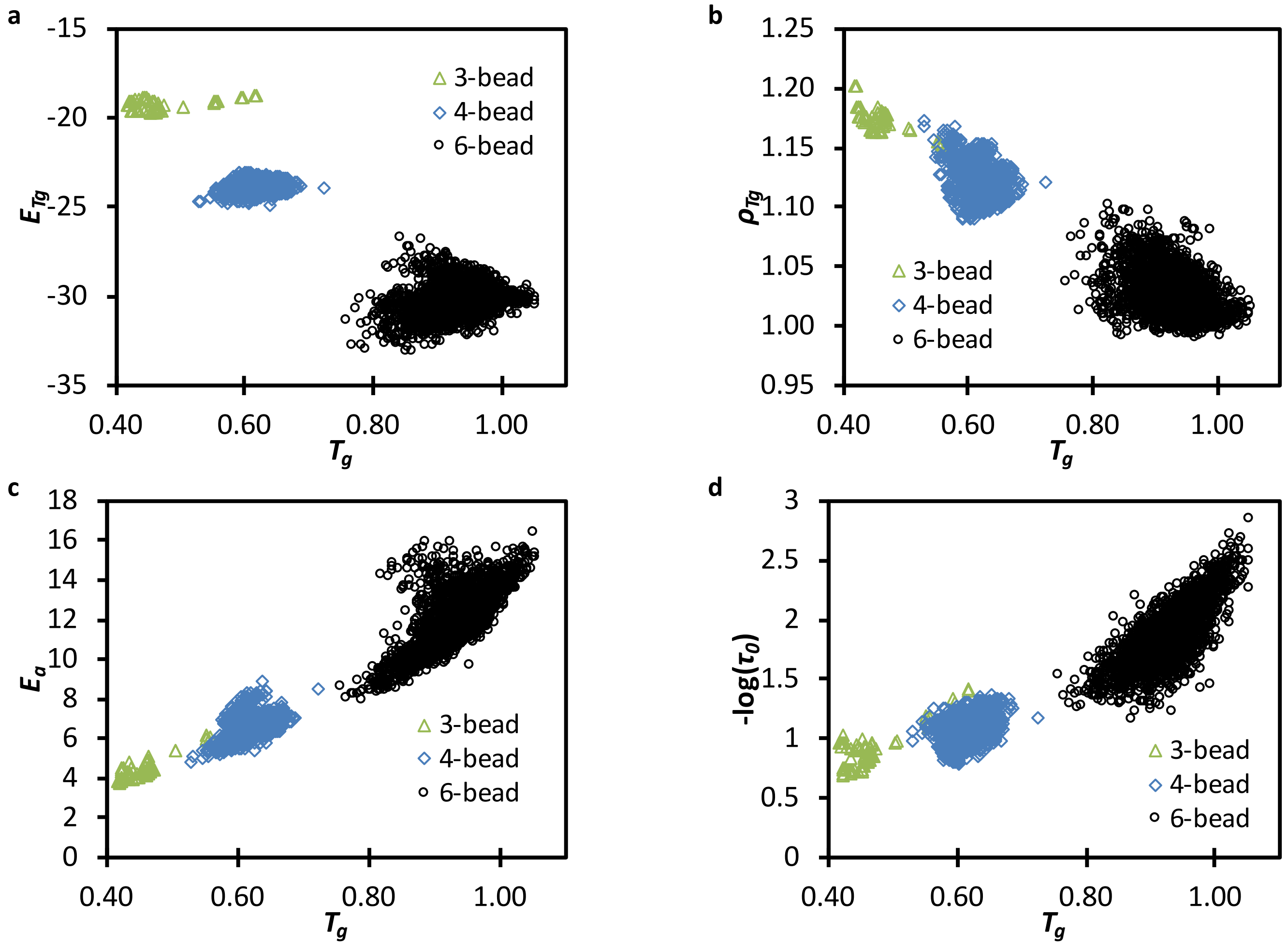

Supplementary Figure 2: Plots comparing various glass formation behaviour descriptors against T_g. a) Dependence of pair energy at extrapolated T_g on T_g. b) Dependence of system density at extrapolated T_g on T_g. c) Dependence of Arrhenius activation energy on T_g. d) Dependence of Arrhenius pre-factor on T_g.

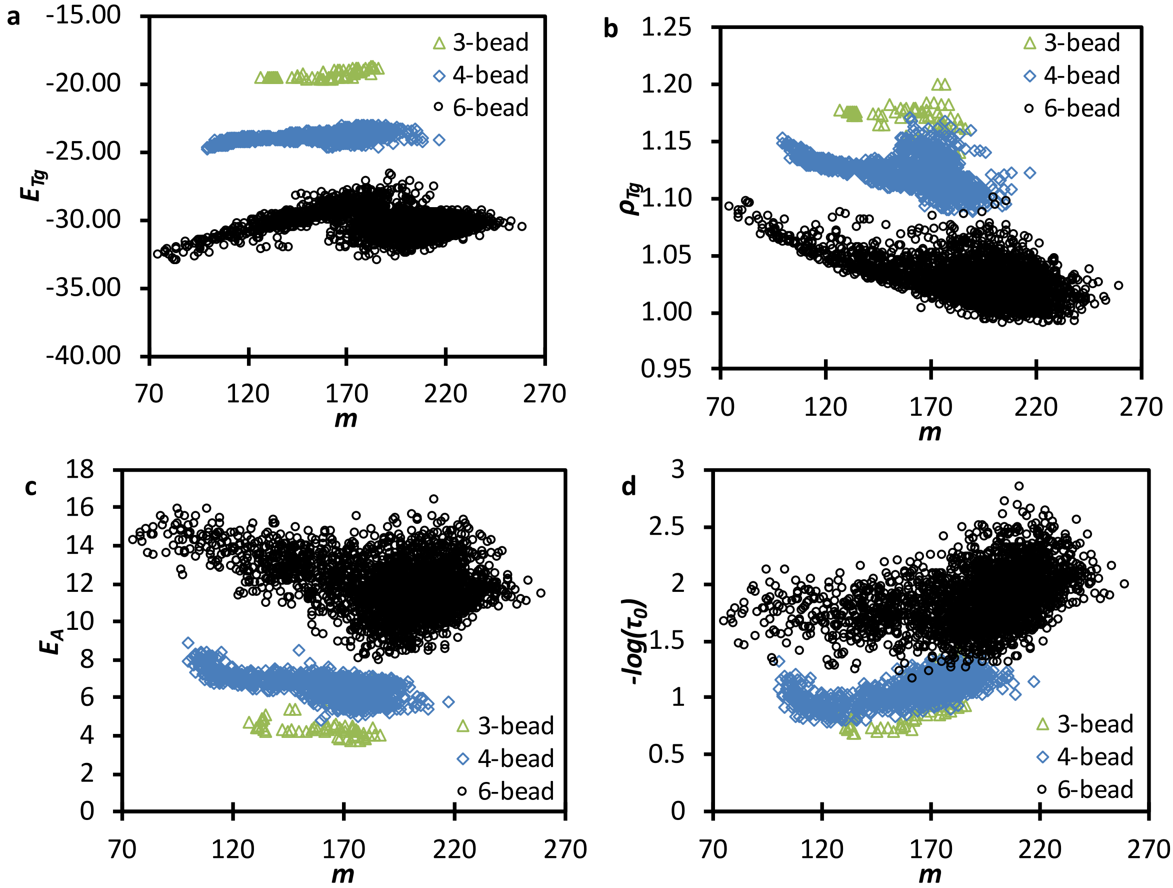

Supplementary Figure 3: Plots comparing various glass formation behaviour descriptors against *m*. a) Dependence of pair energy at extrapolated T_g on *m*. b) Dependence of system density at extrapolated T_g on *m*. c) Dependence of Arrhenius activation energy on *m*. d) Dependence of Arrhenius pre-factor on *m*.

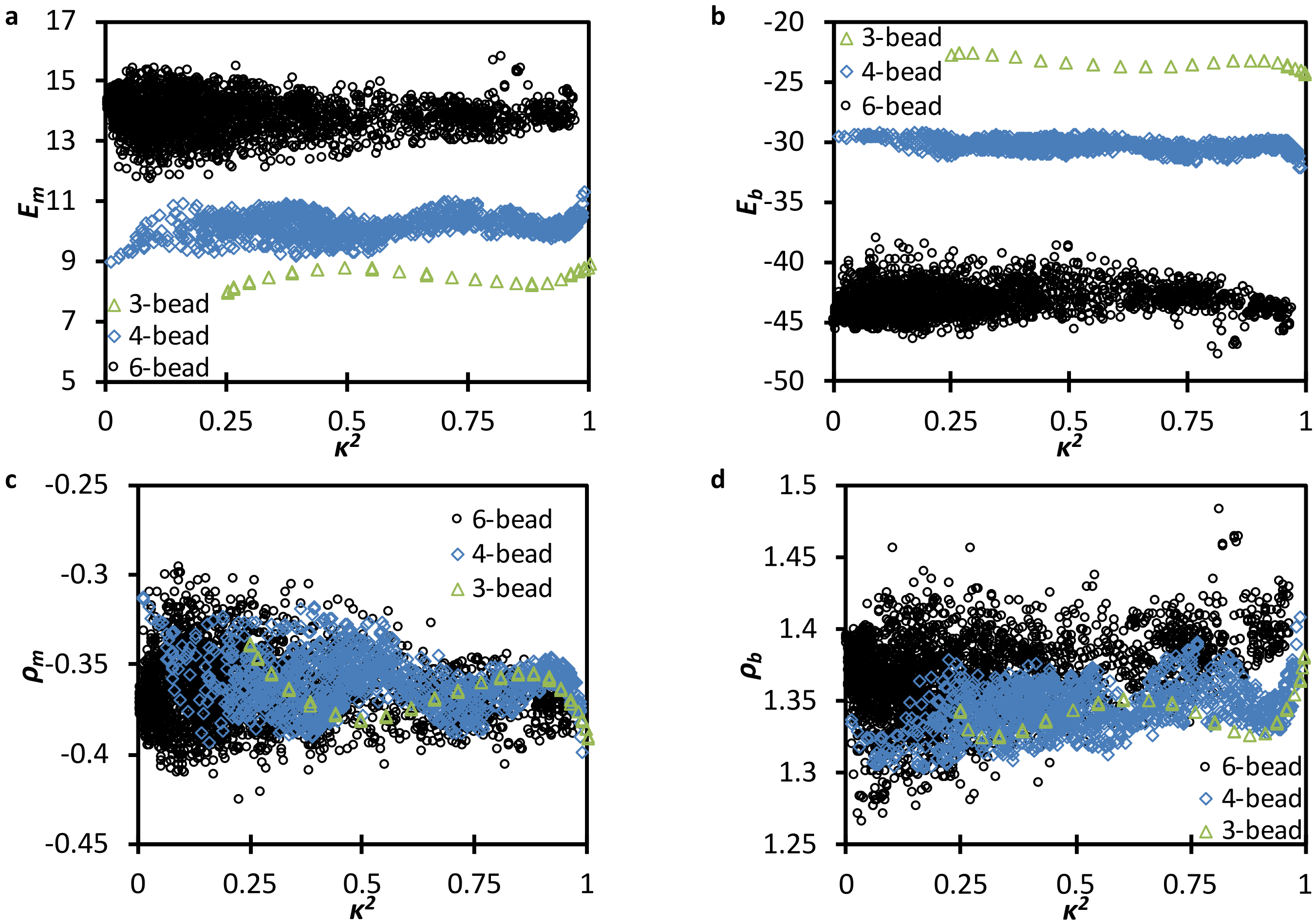

Supplementary Figure 4: Plots comparing various glass formation behaviour descriptors against κ^2. a) Dependence of slope of pair energy vs. temperature on κ^2. b) Dependence of intercept of pair energy vs. temperature on κ^2. c) Dependence of slope of density vs. temperature on κ^2. d) Dependence of intercept of density vs. temperature on κ^2.

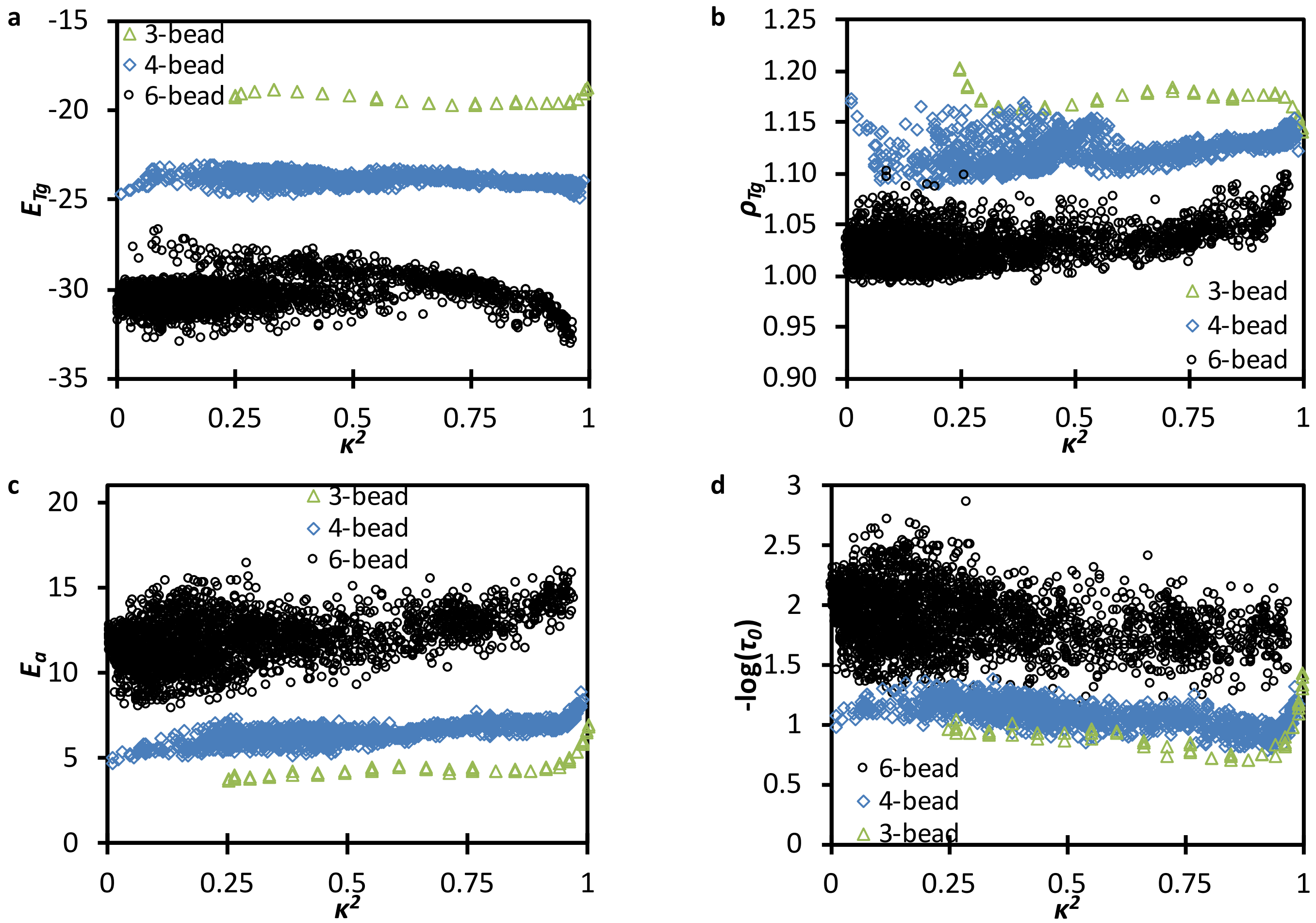

Supplementary Figure 5: Plots comparing various glass formation behaviour descriptors against κ^2. a) Dependence of pair energy at extrapolated T_g on κ^2. b) Dependence of system density at extrapolated T_g on κ^2. c) Dependence of Arrhenius activation energy on κ^2. d) Dependence of Arrhenius pre-factor on κ^2.

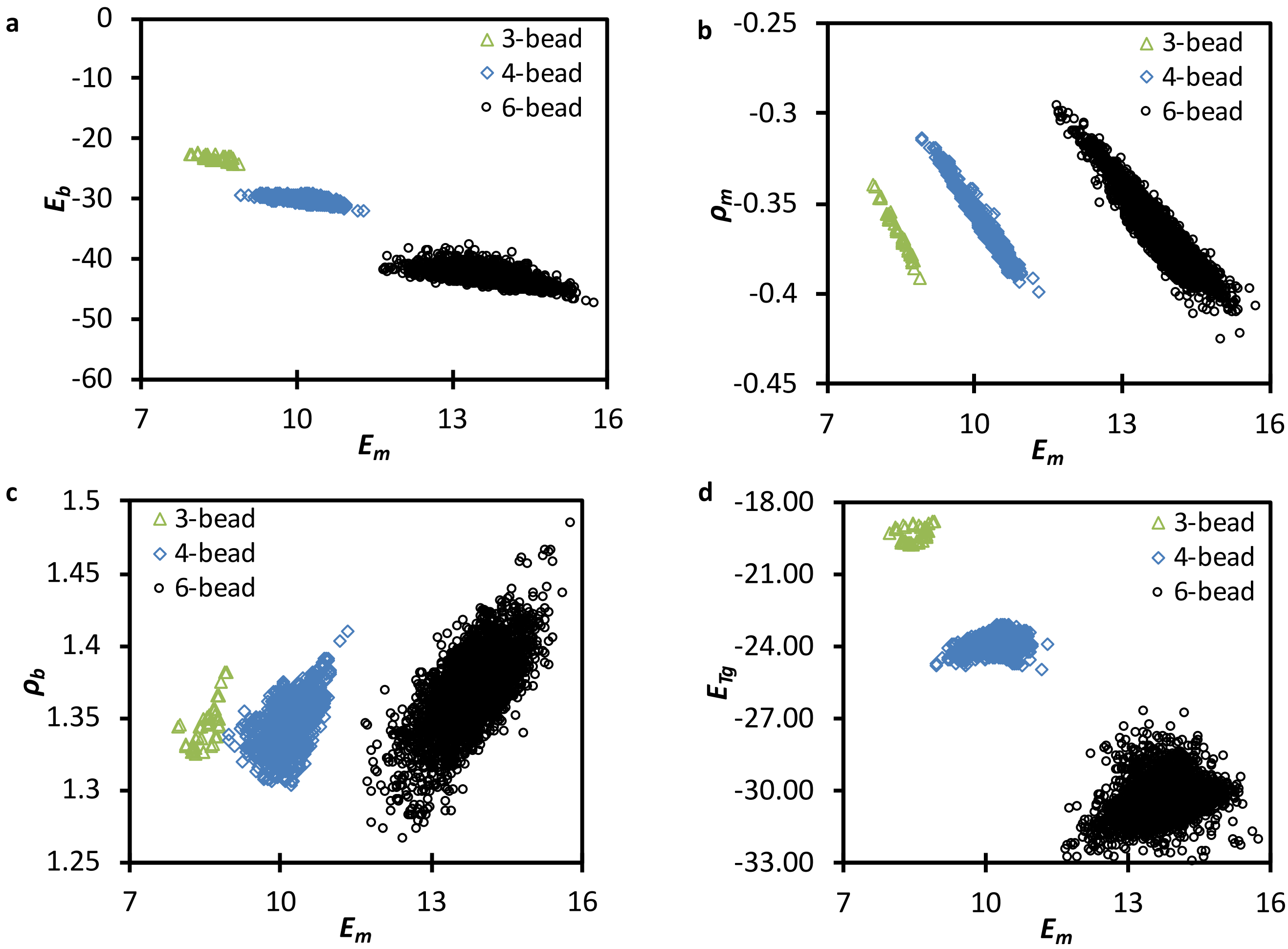

Supplementary Figure 6: Plots comparing various glass formation behaviour descriptors against E_m, slope of pair energy vs. temperature. a) Dependence of intercept of pair energy vs. temperature on E_m. b) Dependence of slope of density vs. temperature on E_m. c) Dependence of intercept of density vs. temperature on E_m. d) Dependence of pair energy at extrapolated T_g on E_m.

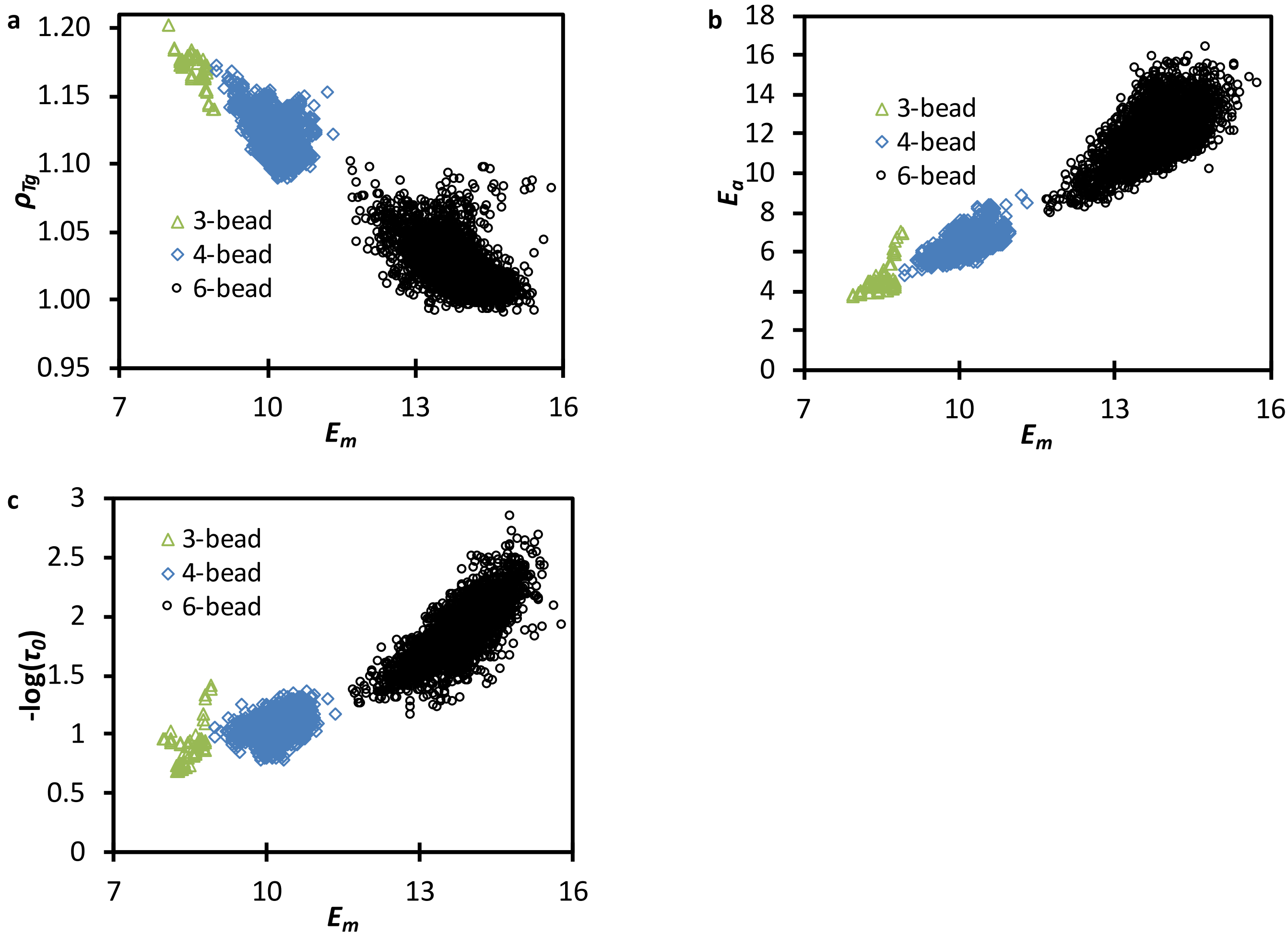

Supplementary Figure 7: Plots comparing various glass formation behaviour descriptors E_m, slope of pair energy vs. temperature. a) Dependence of system density at extrapolated T_g on E_m. b) Dependence of Arrhenius activation energy on E_m. c) Dependence of Arrhenius pre-factor on E_m.

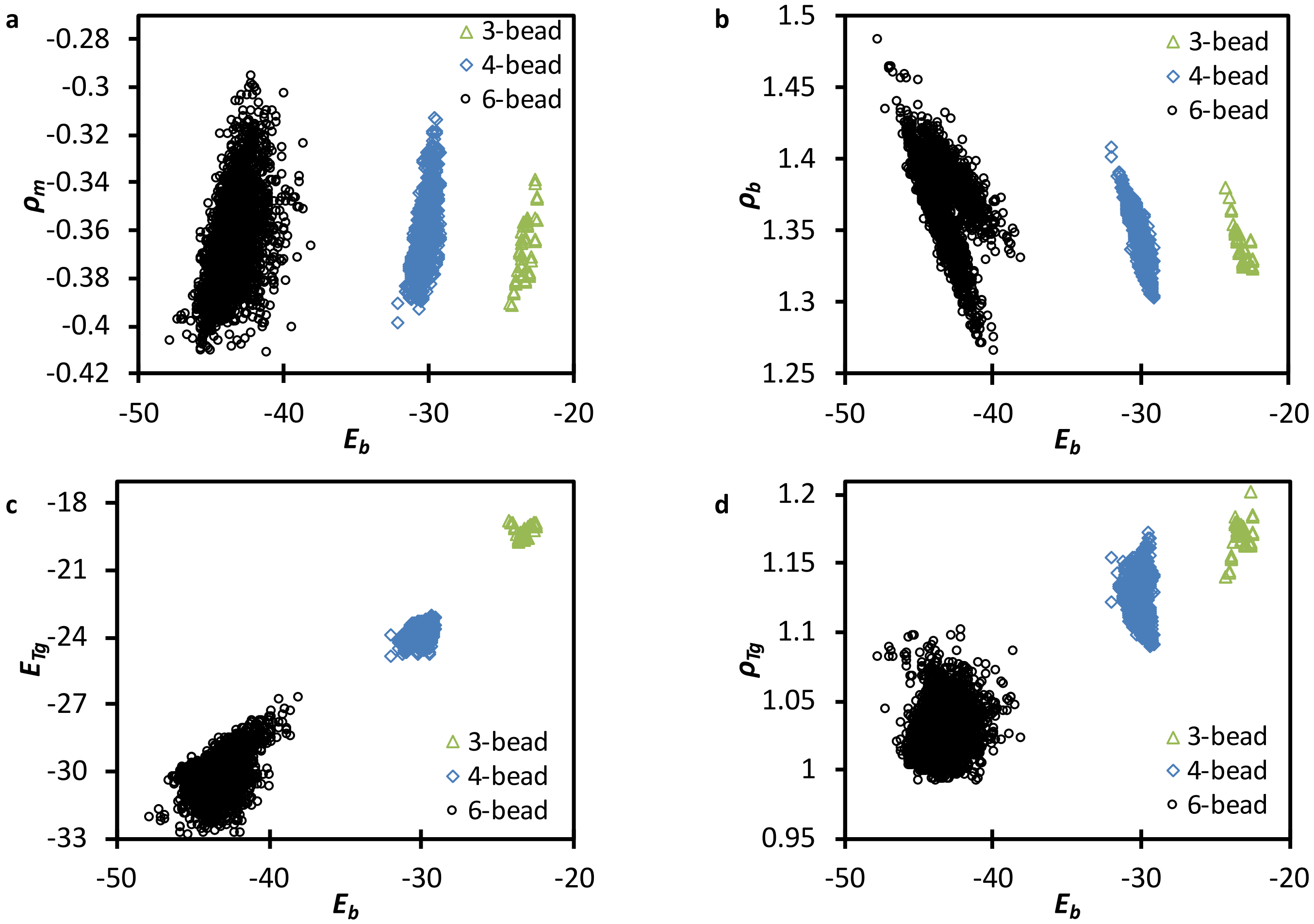

Supplementary Figure 8: Plots comparing various glass formation behaviour descriptors E_b, intercept of pair energy vs. temperature. a) Dependence of slope of density vs. temperature on E_b. b) Dependence of intercept of density vs. temperature on E_b. c) Dependence of pair energy at extrapolated T_g on E_b. d) Dependence of density at extrapolated T_g on E_b.

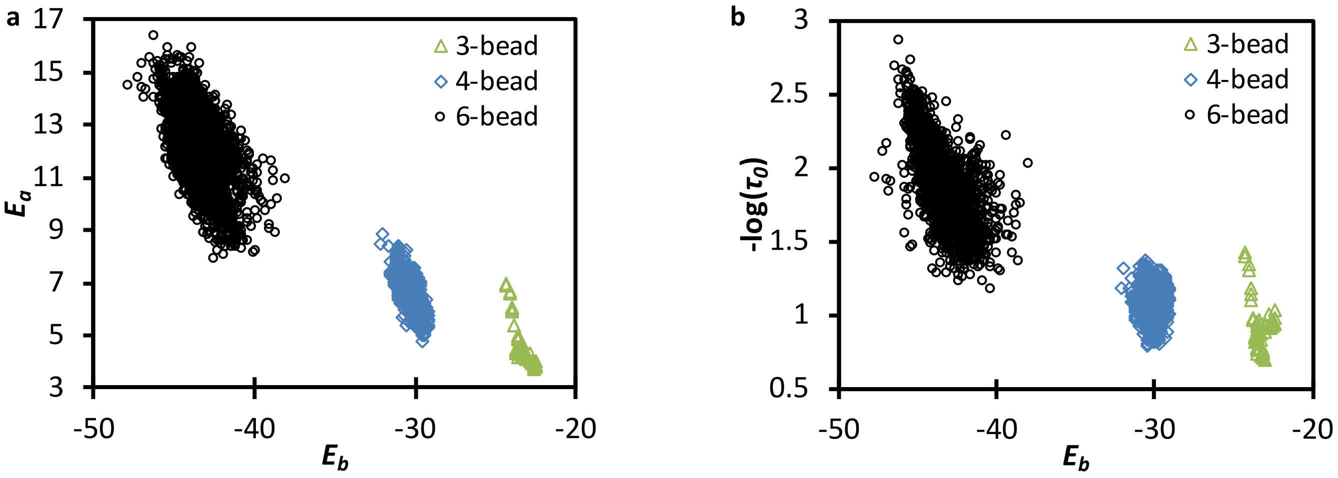

Supplementary Figure 9: Plots comparing various glass formation behaviour descriptors E_b, intercept of pair energy vs. temperature. a) Dependence of Arrhenius activation energy on E_b. b) Dependence of Arrhenius pre-factor on E_b.

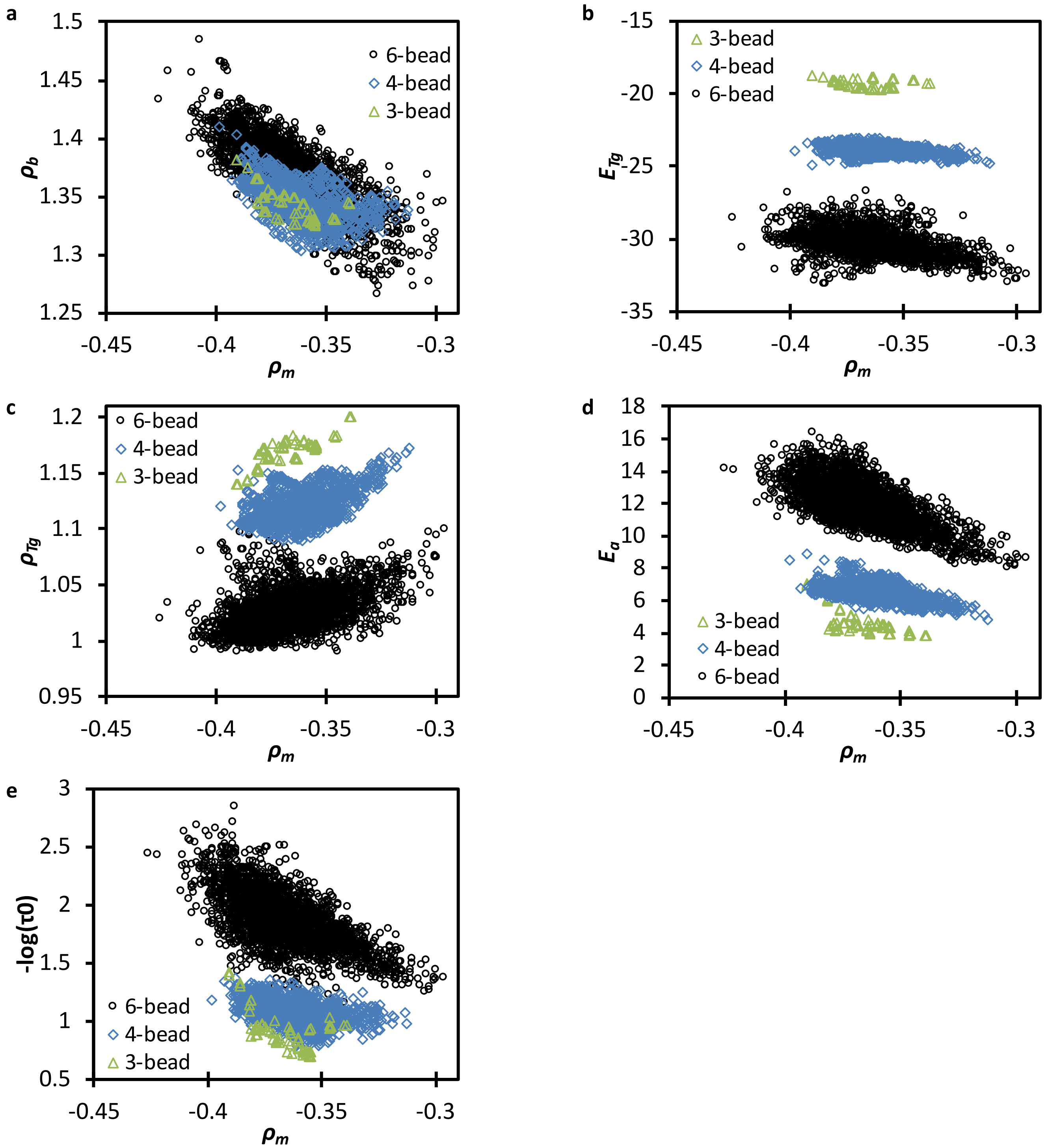

Supplementary Figure 10: Plots comparing various glass formation behaviour descriptors ρ_m, slope of density vs. temperature. a) Dependence of intercept of density vs. temperature on ρ_m. b) Dependence of pair energy at extrapolated T_g on ρ_m. c) Dependence of density at extrapolated T_g on ρ_m. d) Dependence of Arrhenius activation energy on ρ_m. e) Dependence of Arrhenius pre-factor on ρ_m.

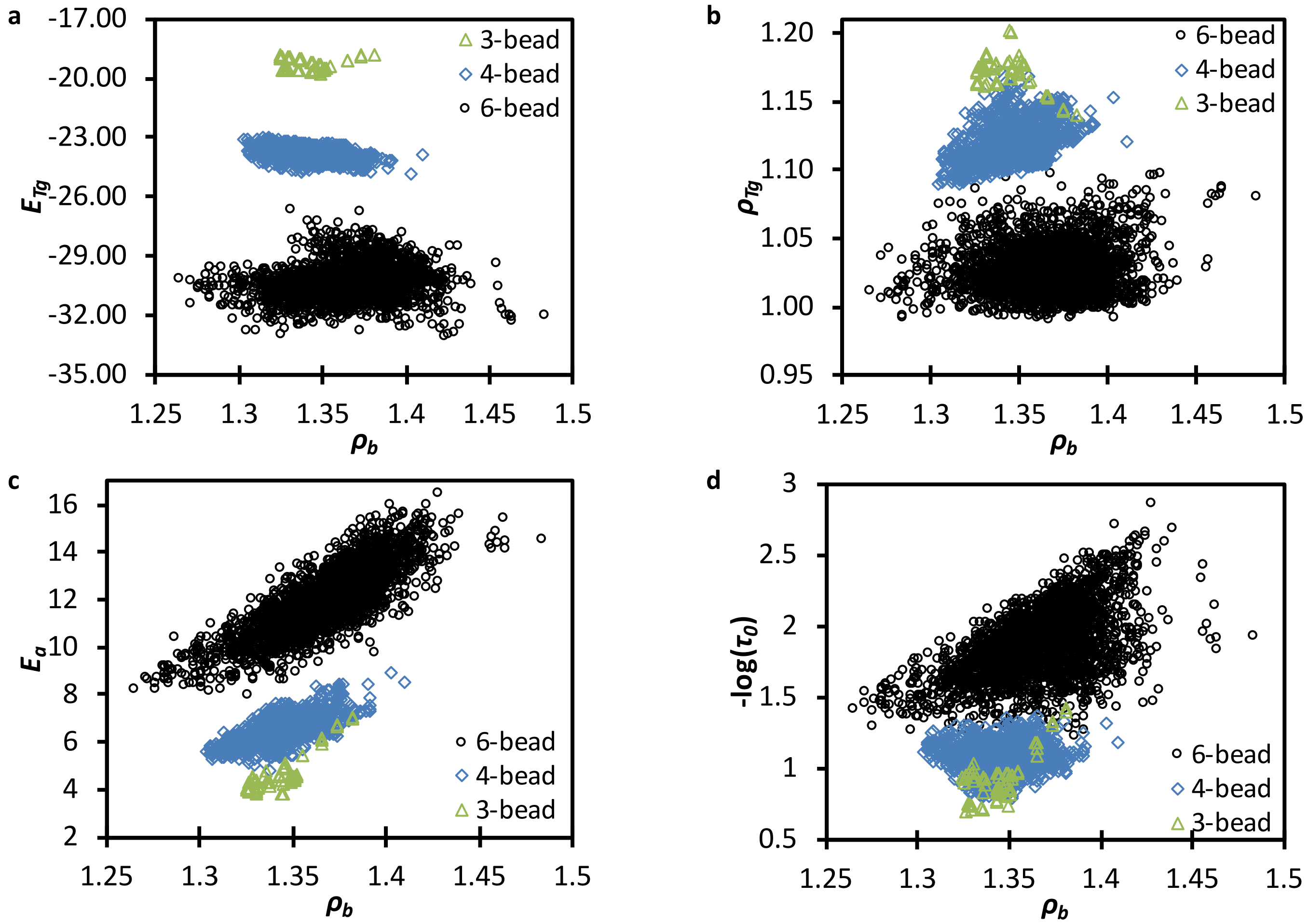

Supplementary Figure 11: a) Dependence of pair energy at extrapolated T_g on ρ_b. b) Dependence of density at extrapolated T_g on ρ_b. c) Dependence of Arrhenius activation energy on ρ_b. d) Dependence of Arrhenius pre-factor on ρ_b.

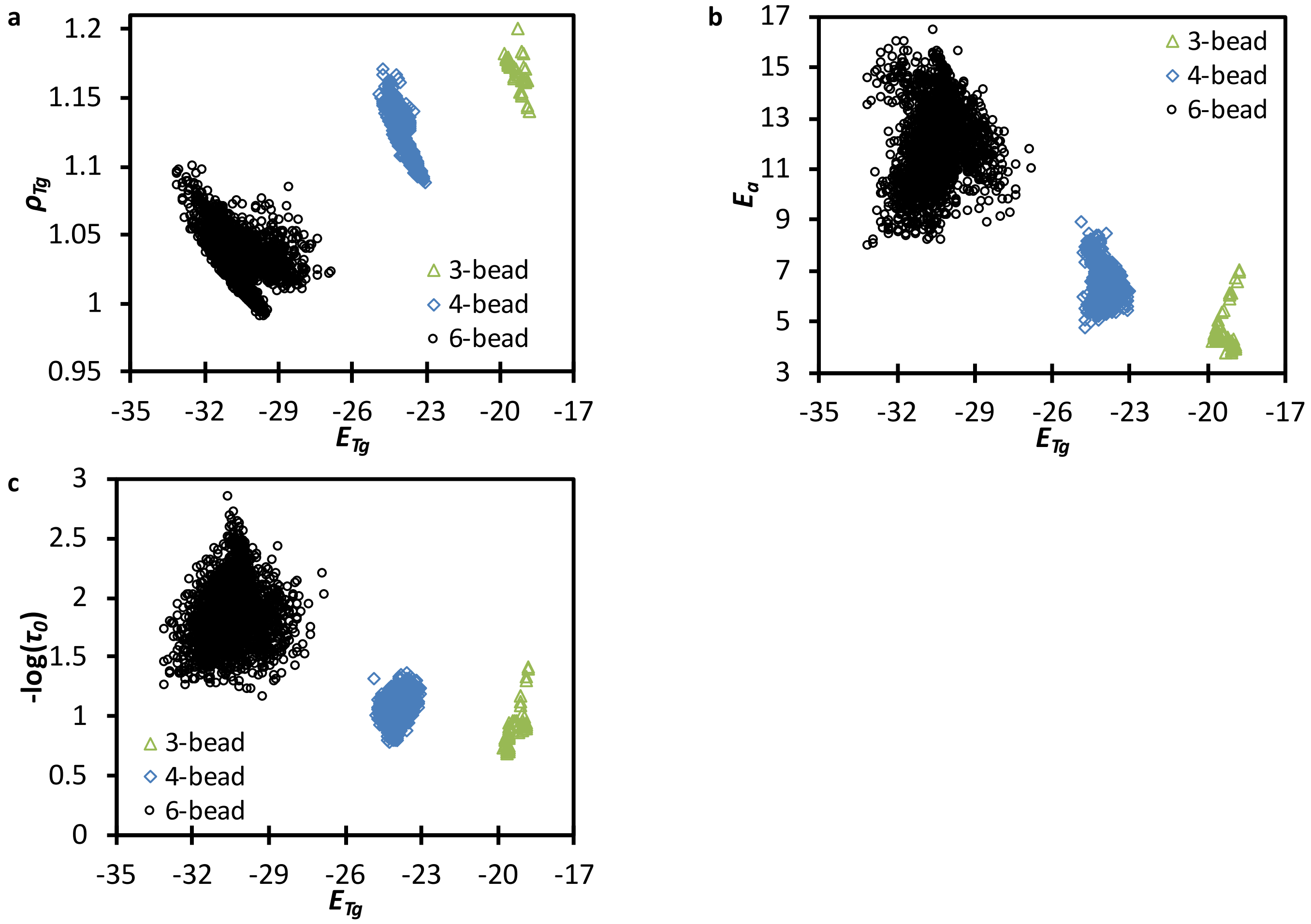

Supplementary Figure 12: a) Dependence of density at extrapolated T_g on E_{Tg}. b) Dependence of Arrhenius activation energy on E_{Tg}. c) Dependence of Arrhenius pre-factor on E_{Tg}.

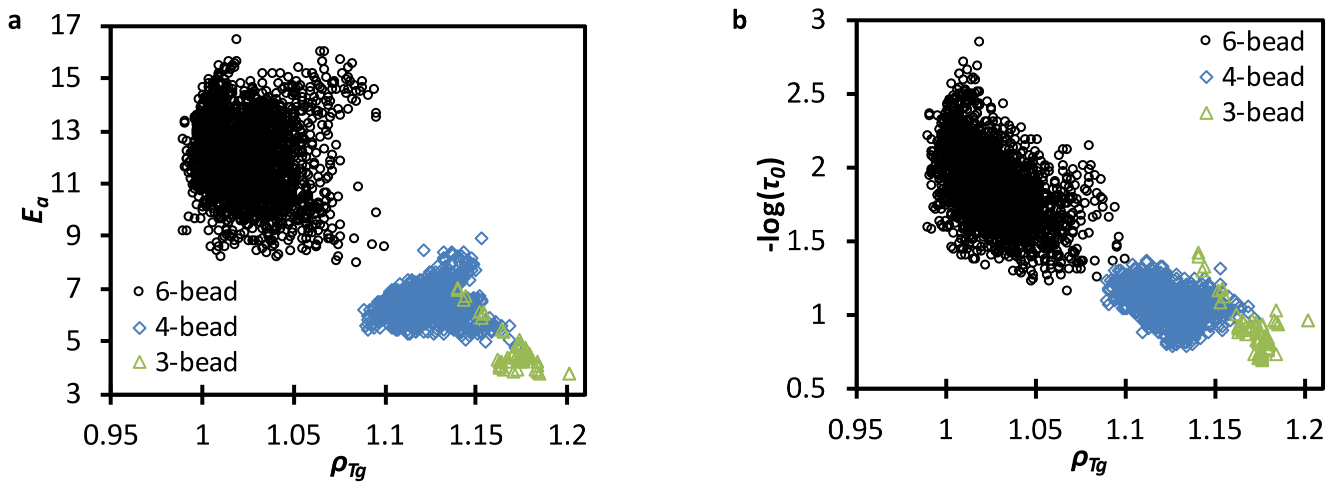

Supplementary Figure 13: a) Dependence of Arrhenius activation energy on ρ_{Tg}. b) Dependence of Arrhenius pre-factor on ρ_{Tg}.

a

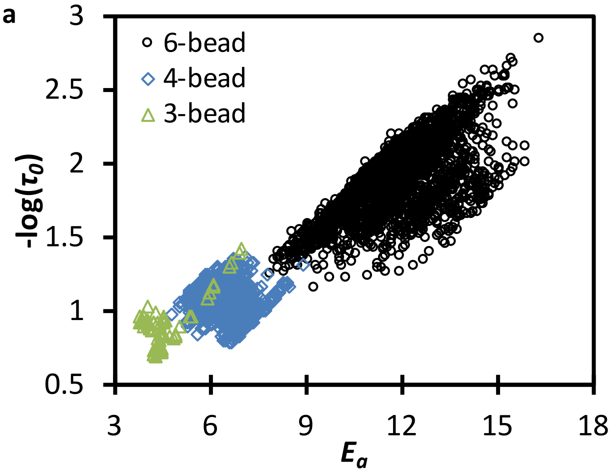

Supplementary Figure 14: a) Dependence of Arrhenius pre-factor on E_a.